A Buckling Problem for Graphene Sheets

J. Galagher[1], *Y. Milman*[2], *S. Ryan*[3], *D. Golovaty*[3], *P. Wilber*[3], *and A. Buldum*[4]

[1] Department of Physics, Rochester Institute of Technology, Rochester, NY 14623, USA
[2] Department of Mathematics, The City College of New York, New York, NY 10031, USA
[3] Department of Theoretical and Applied Mathematics, The University of Akron, Akron, OH 44325, USA
[4] Department of Physics, The University of Akron, Akron, OH 44325, USA

jrg0235@rit.edu, milmann@netzero.net, sdr17@uakron.edu, dmitry@math.uakron.edu, pwilber@math.uakron.edu, buldum@nebula.physics.uakron.edu

ABSTRACT: We develop a continuum model that describes the elastic bending of a graphene sheet interacting with a rigid substrate by van der Waals forces. Using this model, we study a buckling problem for a graphene sheet perpendicular to a substrate. After identifying a trivial branch, we combine analysis and computation to determine the stability and bifurcations of solutions along this branch. Also presented are the results of atomistic simulations. The simulations agree qualitatively with the predictions of our continuum model but also suggest the importance, for some problems, of developing a continuum description of the van der Waals interaction that incorporates information on atomic positions.

Keywords: graphene, elastica model, Lennard-Jones potential, stability analysis

1 Introduction

A graphene sheet is a single-atom-thick layer of carbon atoms in which each atom is bonded to its three nearest neighbors to form a hexagonal lattice. Because stacked graphene sheets are the building blocks of graphite, a naturally occurring form of carbon, there has been a long-standing interest in their mechanical properties. This interest has intensified during the last decade with the explosion of research on carbon nanotubes, which have the structure of a graphene sheet rolled into a cylinder. Numerous studies have demonstrated that carbon nanotubes have remarkable mechanical properties (see [5] for a survey), and it is expected that isolated graphene sheets will share many of these properties. Currently, mechanical and chemical methods are being developed for isolating individual graphene layers [1]–[4].

The general motivation for this work is to develop accurate continuum models of graphene. More specifically, the problem we formulate is driven by recent interest in the fabrication of devices at the nanoscale [6]. Because of their mechanical and electrical properties, graphene sheets may be useful building blocks in a variety of potential nanoscale devices [7]–[9]. However, fabricating such devices may entail the successful mechanical manipulation of individual graphene sheets. One could view our problem as describing part of a nanoscale fabrication process in which a graphene sheet is positioned perpendicularly against a rigid surface. (This positioning could be accomplished by the probe tip of an atomic force microscope [10].) Important for successfully building the device would be to know how hard the sheet can be pushed before buckling into a shape that is no longer perpendicular to the rigid surface.

In this paper, we develop a continuum model of a graphene sheet interacting with a rigid substrate. The graphene sheet is modeled as an elastica. We use a variational approach, in which the energy has two parts, the bending energy of the sheet and the

energy from the interaction of the sheet with the substrate by van der Waals forces. In our continuum model, the van der Waals potential is constructed in such a way that it depends neither on the positions of the atoms on the sheet nor on the positions of the atoms on the substrate. Using the model, we study the buckling of a graphene sheet perpendicular to a rigid substrate. The bottom edge of the sheet approaches the substrate as the top edge of the sheet is loaded by a prescribed force. After identifying a trivial branch of solutions, we combine analysis and computation to study the stability and bifurcations of solutions along this branch.
Also included are the results of atomistic simulations. These simulations agree qualitatively with the predictions of our model. An interesting feature of the atomistic results is a discrete jumping, as opposed to a continuous slipping, of the bottom edge of the buckled sheet across the substrate. Specifically, as the load is increased beyond the buckling load, the sheet's bottom edge jumps between particular atomic locations on the substrate. This phenomena is not predicted by our model, which suggests that a continuum description of van der Waals interaction should be developed that incorporates information on atomic positions.

2 Formulation of Model

We model a substrate as a rigid infinite planar graphene sheet. We assume that interacting with this substrate is a flexible graphene sheet of length L and infinite width. We consider only deformations of the sheet for which its top and bottom edges remain straight and parallel both to the substrate and to each other and for which the deformation is the same in any plane perpendicular to the top and bottom edges. The deformation of a typical cross-section is depicted in Figure 1. A vertical contact force of linear density λ is applied to the top edge, while the bottom edge remains free. For a typical material point $s \in [0, L]$, we let $\theta(s)$ denote the angle that the tangent to the cross-section makes with the horizontal. We denote the distance between the bottom edge of the graphene sheet (which corresponds to $s = 0$) and the substrate by y_0.

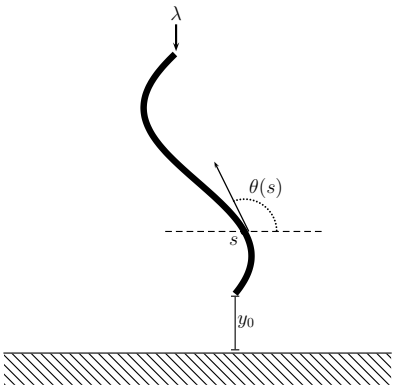

Figure 1: Graphene sheet and substrate.

We approximate the van der Waals energy of interaction between the substrate and the sheet using the Lennard-Jones potential that depends on the distance between the points on two continuum surfaces. (We ignore the self-interactions within each lattice.) Once integrated over the entire substrate, the interaction energy at each point of the sheet depends only on the distance between that point and the substrate. The graph of the van der Waals energy e per unit length along the cross section is shown in Figure 3(a). Note that this profile closely resembles that of the standard 6-12 potential. See [11] for details on the derivation of e.
We note that our approximation to the van der Waals interaction is accurate away from the substrate, but fails at distances near to the equilibrium separation d in Figure 3(b),

where the effects of individual atomic positions begin to be felt. We discuss the consequences of the continuum approximation in the subsequent sections.
The energy of the graphene sheet consists of the bending energy [12] (as in the elastica model [13]) supplemented with the potential energy of interaction with the substrate

$$E[\theta, y_0] = \int_0^L \left(\frac{\beta}{2} \left(\theta'\right)^2 + e\left(y_0 + \int_0^s \sin\theta \, d\sigma \right) \right) ds, \tag{1}$$

where β is the bending constant and e is the energy density of the van der Waals interaction. The distance between the point corresponding to the arclength s and the substrate is $y_0 + \int_0^s \sin\theta \, d\sigma$. Note that the shape of the sheet is completely determined once y_0 and θ are known.
The graphene sheet is vertical if $\theta \equiv \pi/2$. The energy of the perturbed configuration $(y_0 + \delta y_0,\ \pi/2 + \delta\theta)$ is given by

$$E[\pi/2+\delta\theta, y_0+\delta y_0] = \int_0^L \left(\frac{\beta}{2} \left(\delta\theta'\right)^2 + e\left(y_0 + \delta y_0 + \int_0^s \cos(\delta\theta) d\sigma \right) \right) ds. \tag{2}$$

The potential energy due to an external force of the linear density λ applied at the top of the sheet is

$$W[\delta\theta, \delta y_0] = -\lambda \left(\delta y_0 + \int_0^L \cos(\delta\theta) d\sigma - L \right). \tag{3}$$

Then the total potential energy $E + W$ of the perturbed configuration is

$$\begin{aligned} F[\delta\theta, \delta y_0] := \int_0^L \left(\frac{\beta}{2} \left(\delta\theta'\right)^2 + e\left(y_0 + \delta y_0 + \int_0^s \cos(\delta\theta) d\sigma \right) \right) ds \\ -\lambda(\delta y_0 + \int_0^L \cos(\delta\theta) d\sigma - L). \end{aligned} \tag{4}$$

By linearizing F near $\delta y_0 = 0,\ \delta\theta \equiv 0$, we obtain a force balance condition

$$\lambda = e(y_0 + L) - e(y_0). \tag{5}$$

(Note that $\theta = \pi/2$ already satisfies the appropriate Euler-Lagrange equation.)
The stability of the vertical solution can be deduced from the second variation of the potential energy. Collecting the second-order terms in the expansion of F with respect to δy_0 and $\delta\theta$ and integrating by parts in (2), we obtain

$$\begin{aligned} G[\delta\theta, \delta y_0] := \frac{1}{2} \int_0^L \left(\beta(\delta\theta')^2 + [e(y_0 + s) - e(y_0)]\delta\theta^2 \right) ds \\ + \frac{\delta y_0^2}{2} [e'(y_0 + L) - e'(y_0)]. \end{aligned} \tag{6}$$

3 Stability Analysis

A vertical solution exists exactly when the contact force λ applied at the top of the sheet and the position y_0 of the bottom of the sheet satisfy (5). Figure 2 shows the curve of points satisfying (5) in the $\lambda\, y_0$-plane for a typical value of L. This curve represents the vertical solutions, which corresponds to our trivial branch, whose bifurcations and stability we analyze next.
We define a solution on the vertical branch to be stable if the second variation (6) is

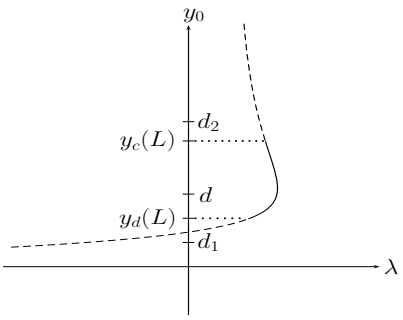

Figure 2: Branch of vertical solutions

positive semi-definite, i.e., is non-negative for every combination of $\delta\theta$ and δy_0.

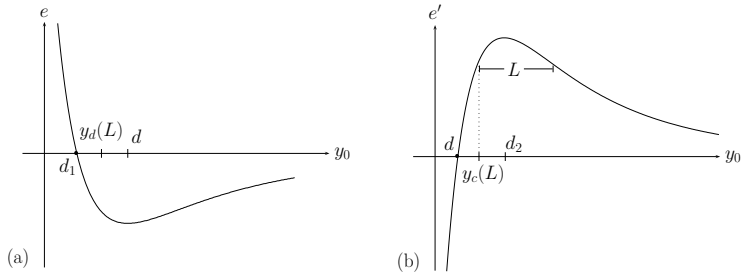

Figure 3: (a) Graph of energy e per unit length. (b) Graph of e'

First we claim that, given L, there is a $y_c(L)$ such that any solution on the vertical branch with $y_0 > y_c(L)$ is unstable. This is easily verified by examining Figure 3(b), from which one sees that if $y_0 > y_c(L)$, then $e'(y_0 + L) - e'(y_0) < 0$. Hence the second variation G can be made negative by choosing $\delta\theta \equiv 0$, which makes the integral term in (6) vanish, and by choosing any $\delta y_0 \neq 0$. Note from Figure 3(b) that $y_c(L) > d$. Also, $y_c(L) \to d_2$, the point at which e' attains its maximum, as $L \to 0$, and $y_c(L) \to d$ as $L \to \infty$.

Next we claim that, given L, there is a $y_d(L)$ such that any solution on the vertical branch with $y_0 < y_d(L)$ is unstable. We define $g(y_0) = \int_0^L [e(y_0 + s) - e(y_0)]\, ds$. Using Figure 3(a), one checks that $g(y_0) < 0$ for $y_0 < d_1$, that $g(y_0) > 0$ for $y_0 > d$, and that $g'(y_0) > 0$ for $d_1 \leq y_0 \leq d$. It follows that there exists a unique value $y_d(L)$ with $d_1 < y_d(L) < d$ such that $g(y_0) < 0$ for $y_0 < y_d(L)$ and $g(y_0) > 0$ for $y_0 > y_d(L)$. For $y_0 < y_d(L)$, we can choose $\delta y_0 = 0$ and $\delta\theta$ equal to any non-zero constant function to make (6) negative, so that the solution corresponding to this y_0 is unstable. Also, straightforward arguments show that $y_d(L) \to d$ as $L \to 0$ and that $y_d(L) \to d_1$ as $L \to \infty$.

The arguments above show that any stable solutions on the vertical branch can occur only for y_0 between $y_d(L)$ and $y_c(L)$. Consider y_0 between d and $y_c(L)$. From Figure 3(b) we see that $e'(y_0 + L) - e'(y_0) \geq 0$, while from Figure 3(a) we see that $e(y_0 + s) - e(y_0) \geq 0$ for all $0 \leq s \leq L$. Therefore the second variation is non-negative for any $\delta\theta$ and δy_0, which implies that the corresponding vertical solution is stable.

The stability of solutions on the part of the vertical branch corresponding to y_0 between $y_d(L)$ and d is less readily analyzed. However the problem can be tackled

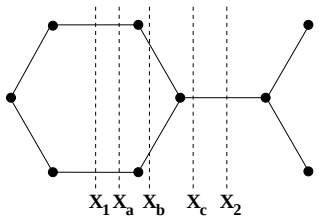

Figure 4: Unit cell of the substrate. The projections of the flexible sheet onto the substrate are labeled for various initial positions.

numerically by finding the smallest value of λ that guarantees the existence of a nontrivial solution to the Euler-Lagrange equation

$$-\beta\delta\theta'' + \left(e\left(y_0 + s\right) - e\left(y_0\right)\right)\delta\theta = 0 \tag{7}$$

for the functional G defined in (6) when $\delta y_0 = 0$. Here $\delta\theta$ satisfies the natural boundary conditions

$$\delta\theta'(L) = \delta\theta'(0) = 0, \tag{8}$$

and λ and y_0 are related via (5). We discretize the second derivative term in (8) by using central differences and find the smallest value of $\lambda > 0$ for which the determinant of the matrix of coefficient vanishes. This procedure yields a bifurcation point slightly larger than $y_d(L)$.

4 Atomistic Modeling

To qualitatively verify the results of the continuum modeling, we use Accelrys Cerius^2 software to create an atomistic model of our system. We fix several rows of atoms at the top edge of the flexible sheet and move them toward the substrate by 0.01 nm per step. After each step, we minimize the energy and find the applied force by using the standard relationship $f = -e'$.

We do not study the influence of relative orientations of the substrate lattice and the flexible sheet lattice and assume that these orientations remain fixed (Figure 4). However we investigate the effect of placing the flexible sheet at different initial position with respect to the substrate unit cell. Figure 5(a) shows the dependence of the total energy on the displacement of the top edge of the flexible sheet from its initial position. The stability loss occurs at the points of rapid drop of the energy with the largest drop corresponding to the onset of deformation in a perfectly vertical sheet. Notice the strong dependence of the stability threshold on the initial placement of the flexible sheet—this effect is lost in our continuum model, which does not take into account positions of individual atoms. Another effect that cannot be described within the same continuum theory is shown in Figure 5(b). As the load is being increased, the successive configurations seem to "snap" from one equilibrium to the next in order to conform to the existing atomic structure of the substrate. Thus the comparison with the atomistic model demonstrates the need to incorporate the individual atomic positions into the continuum description.

Acknowledgments

This work was supported by NSF Grants DMS-04-07361 and DMS-03-54022.

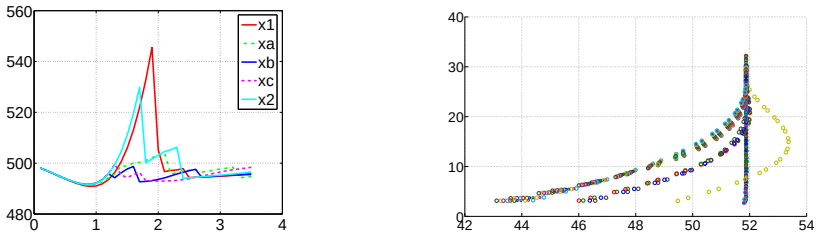

Figure 5: (a) Total energy as a function of initial position of graphene sheet. (b) Successive configurations of the sheet during incremental loading.

References

[1] H. C. Schniepp, J. Li, M. J. McAllister, H. Sai, M. Herrera-Alonso, D. H. Adamson, R. K. Prud'homme, R. Car, D. A. Saville, and I. A. Aksay. Functionalized single graphene sheets derived from splitting graphite oxide. *The Journal of Physical Chemistry Letters B*, 110:8535–8539, 2006.

[2] A.M. Affoune, B. L. V. Prasad, H. Sato, T. Enoki, Y. Kaburagi, and Y. Hishiyama. Experimental evidence of a single nano-graphene. *Chemical Physics Letters*, 348:17–20, 2001.

[3] S. Horiuchi, T. Gotou, M. Fujiwara, T. Asaka, T. Yokosawa, and Y. Matsui. Single graphene sheet detected in a carbon nanofilm. *Applied Physics Letters*, 84(13):2403–2405, 2004.

[4] J. Wang, M. Zhu, R. A. Outlaw, X. Zhao, D. M. Manos, and B. C. Holloway. Synthesis of carbon nanosheets by inductively coupled radio-frequency plasma enhanced chemical vapor deposition. *Carbon*, 42:2867–2872, 2004.

[5] M.-F. Yu. Fundamental mechanical properties of carbon nanotubes: Current understanding and the related experimental studies. *J. of Eng. Mat. and Tech.*, 126:271–278, 2004.

[6] X.-S. Wang. Nanoparticles, nanorods, and other nanostructures assembled on inert surfaces. In *Molecular Building Blocks for Nanotechnology*. Springer, 2007.

[7] M.T. Cuberes. Ultrasonic machining at the nanometer scale. *J. of Phys.: Conference Series*, 61(1):219–223, 2007.

[8] J. Zhou, Z. Shen, S. Hou, X. Zhao, Z. Xue, and Z. Shi, Z. Gu. Adsorption and manipulation of carbon onions on highly oriented pyrolytic graphite studied with atomic force microscopy. *Appl. Surf. Sci.*, 253:3237–3241, 2007.

[9] X. Lu, M. Yu, H. Huang, and R. Ruoff. Tailoring graphite with the goal of achieving single sheets. *Nanotechnology*, 10:269–272, 1999.

[10] J.D. LeGrange. Microscopic manipulation of materials by atomic force microscopy. *Biophys. J.*, 64:903–904, 1993.

[11] J.P. Wilber, A. Buldum, C.B. Clemons, D.D. Quinn, and G.W. Young. Continuum and atomistic modeling of interacting graphene layers. *Phys. Rev. B*, 75:045418, 2007.

[12] M. Arroyo and T. Belytschko. Finite crystal elasticity of carbon nanotubes based on the exponential Cauchy-Born rule. *Phys. Rev. B*, 69:115415–1–11, 2004.

[13] S. S. Antman. *Nonlinear Problems of Elasticity*. Springer, 2005.